

Optical nonreciprocity in rotating diamond with nitrogen-vacancy center

Hong-Bo Huang,¹ Jun-Jie Lin,¹ Yi-Xuan Yao,¹ Ke-Yu Xia,² Zhang-Qi Yin,³ and Qing Ai^{1,*}

¹*Department of Physics, Applied Optics Beijing Area Major Laboratory,
Beijing Normal University, Beijing 100875, China*

²*National Laboratory of Solid State Microstructures,
Collaborative Innovation Center of Advanced Microstructures, College of Engineering and Applied Sciences,
and School of Physics, Nanjing University, Nanjing 210093, China*

³*Center for Quantum Technology Research and Key Laboratory of
Advanced Optoelectronic Quantum Architecture and Measurements (MOE),
School of Physics Beijing Institute of Technology Beijing 100081, China*

(Dated: September 9, 2021)

We theoretically propose a method to realize optical nonreciprocity in rotating nano-diamond with a nitrogen-vacancy (NV) center. Because of the relative motion of the NV center with respect to the propagating fields, the frequencies of the fields are shifted due to the Doppler effect. When the control and probe fields are incident to the NV center from the same direction, the two-photon resonance still holds as the Doppler shifts of the two fields are the same. Thus, due to the electromagnetically-induced transparency (EIT), the probe light can pass through the NV center nearly without absorption. However, when the two fields propagate in opposite directions, the probe light can not effectively pass through the NV center as a result of the breakdown of two-photon resonance.

I. INTRODUCTION

Optical nonreciprocity happens when Lorentz's reciprocity is broken, and it leads to different transmittance when two beams of light propagate in the opposite directions [1]. Optical nonreciprocity plays an important role in optical devices such as isolators and circulators [2], which have further application in quantum networks [3, 4], quantum noise reduction [5], quantum signal processing [6, 7], and photon blockade [8–10]. Traditional nonreciprocity is mainly realized by magneto-optical effect [11–13], which often requires such large size that it is difficult to be used on chips. To overcome this shortcoming, alternative strategies are explored to achieve nonreciprocity, including nonlinear optics [14–16], synthetic magnetism [11, 17, 18], optomechanical coupling [19–21], and non-trivial topology [22]. Interestingly, it has been shown that nonreciprocal transport can also be realized by the irregular thermal motion of atoms [23–26].

In 1961, Fano pointed out that if several different atomic transitions are coupled, the total transition probability will be coherently enhanced or cancelled due to interference of the amplitudes of these transitions [27]. Inspired by this discovery, many studies on atomic coherence appeared, e.g. electromagnetically induced transparency (EIT) [28]. In EIT, adding a strong control field can make the probe light transparent, which will be resonantly absorbed by the atomic medium in the absence of the control field [29]. Because it has a wide range of prospective applications, e.g. nonreciprocal transmission and memory of nonclassical fields [30, 31], EIT has been successfully realized in many systems, such as gas-phase

atoms [32, 33], photosynthetic energy transfer [34, 35], metamaterial [36], superconducting system [37], and NV center in diamond [38].

On the other hand, nitrogen-vacancy (NV) center in diamond is an intriguing platform for quantum information processing [39–41] and quantum sensing [42, 43]. NV center is a pair of point defects at adjacent sites in diamond crystal. Due to long coherence time and easy manipulation at room temperature, it has been shown that it can be utilized for detecting magnetic cluster [44], state transfer by shortcut to adiabaticity [45–47], gyroscope [48, 49], and quantum hyperbolic metamaterial [50]. Recently, it has been experimentally realized that nanoparticles levitated in vacuum can rotate at a frequency of GHz [51–53]. Inspired by the rapid progress on the quantum coherent devices by NV centers, a question naturally comes to our mind: Can we make use of a rotating diamond with NV centers for realizing optical nonreciprocity?

In this paper, we propose a non-reciprocal transmission based on a rotating nano-diamond at a high speed. The nano-diamond doped with NV centers is placed in an optical cavity. Two electronic ground states and one electronic excited state of the NV center form a Λ -type three-level configuration and the optical transitions between the ground and excited states can be induced by electromagnetic fields, i.e., the control field and cavity field. We explore the transmittance of the probe light incident in different directions with respect to the control field.

The paper is organized as follows: In Sec. II, we first introduce the model of the system and we derive the expressions of the transmittance at the steady state by the Heisenberg-Langevin approach. In Sec. III, we numerically show the transmittance for the two cases and analyze the results by the dark-state mechanism in Ref. [38]. Finally, we discuss the prospect of our proposal and sum-

*Electronic address: aiqing@bnu.edu.cn

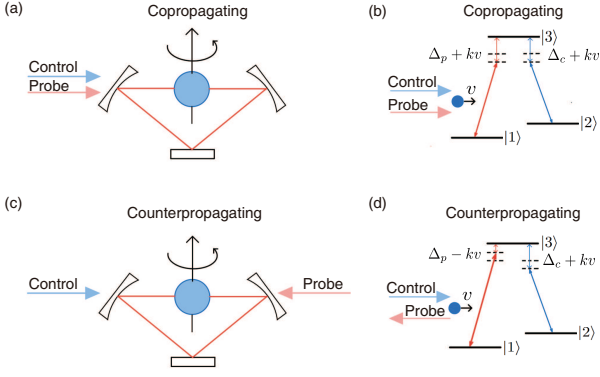


Figure 1: Schematic diagram of optical nonreciprocity in a rotating nano-diamond with an NV center. (a) and (c) are the cases when the probe and the control field propagate in the same/opposite direction, respectively. A high-speed rotating nano-diamond is placed in an optical cavity. After the lights entering the cavity, they are coupled with the NV center in the nano-diamond. (b) and (d) are energy-level diagrams for (a) and (c), respectively. Due to the relative motion between the NV center and the lights, different Doppler shifts are induced. When the laser and NV center move along the same direction, the Doppler shift is $\Delta + kv$. Otherwise, the Doppler shift is $\Delta - kv$.

marize the main findings in Sec. IV.

II. THEORETICAL MODEL

We consider a rapidly-rotating nano-diamond with an NV center in an optical cavity, as illustrated in Fig. 1. A beam of control light and probe light respectively interact with the optical transitions at $\lambda = 637.2$ nm of an NV center from the electronic ground state $|\pm 1\rangle$ to the electronic excited state $|A_2\rangle$ [45, 50]. The cavity mode with resonance frequency ω_a is coupled to the transition $|1\rangle(\equiv | + 1\rangle) \leftrightarrow |3\rangle(\equiv |A_2\rangle)$ with Rabi frequency g . Moreover, there is a probe laser injected into the cavity. A strong control laser beam with a carrier frequency ω_c and Rabi frequency Ω_c is coupled to the transition $|2\rangle(\equiv | - 1\rangle) \leftrightarrow |3\rangle$.

The relative motion between NV center and photons gives rise to the microscopic Doppler shift, i.e., $\omega_\alpha - \vec{k}_\alpha \cdot \vec{v}$. Here, ω_α ($\alpha = a, c$) is the frequency of the photon experienced by the NV center when the latter is at rest. \vec{k}_α is the wave vector of the light in the nano-diamond and \vec{v} is the velocity of the NV center. For example, if the NV center and light move in the same direction, the frequency of the photon experienced by the NV center becomes $\omega - kv$.

Assuming $\hbar = 1$, the Hamiltonian of the system takes

the following form

$$\begin{aligned}
 H = & \omega_a a^\dagger a + \omega_p a_p^\dagger a_p + \sum_{l=1}^3 \omega_l \sigma_{ll} + \sum_r \omega_r d_r^\dagger d_r \\
 & + \sum_q \omega_q b_q^\dagger b_q + \Omega_c e^{i(\omega_c - \vec{k}_c \cdot \vec{v})t} \sigma_{23} + g e^{-i\vec{k}_a \cdot \vec{v}t} a^\dagger \sigma_{13} \\
 & + i\sqrt{\kappa_1} a^\dagger a_p + \sum_r g_r d_r^\dagger a + \sum_q (g_{1q} \sigma_{31} + g_{2q} \sigma_{32}) b_q \\
 & + \text{h.c.}, \tag{1}
 \end{aligned}$$

where ω_l ($l = 1, 2, 3$) is the energy of state $|l\rangle$, and $\hat{\sigma}_{lm} = |l\rangle\langle m|$ is the operator of NV center, a and a_p are respectively the annihilation operator of the cavity mode and the probe field, Ω_c is the Rabi frequency of the control field with frequency ω_c and wave vector \vec{k}_c , g is the Rabi frequency of the cavity mode with frequency ω_a and wave vector \vec{k}_a . b_q and d_r are annihilation operator of the reservoir interacting with the NV center and cavity respectively, where ω_q and ω_r are the frequency of the corresponding harmonic oscillator. g_r , g_{1q} , and g_{2q} correspond to the coupling strength between the reservoir and the cavity, atomic transition $|1\rangle \leftrightarrow |3\rangle$, and $|2\rangle \leftrightarrow |3\rangle$, respectively.

By using the unitary transformation

$$\begin{aligned}
 U = & \exp\{i[\omega_p a^\dagger a + \omega_p a_p^\dagger a_p + \sum_r \omega_r d_r^\dagger d_r \\
 & + \sum_q \omega_q b_q^\dagger b_q + (\omega_3 - \omega_p + \vec{k}_a \cdot \vec{v})\sigma_{11} \\
 & + (\omega_3 - \omega_c + \vec{k}_c \cdot \vec{v})\sigma_{22} + \omega_3 \sigma_{33}]t\}, \tag{2}
 \end{aligned}$$

we can obtain the Hamiltonian in the interaction picture as

$$\begin{aligned}
 H_I = & \Delta_a a^\dagger a + (\Delta_p + \vec{k}_a \cdot \vec{v})\sigma_{11} + (\Delta_c + \vec{k}_c \cdot \vec{v})\sigma_{22} \\
 & + \Omega_c \sigma_{32} + g a^\dagger \sigma_{13} + i\sqrt{\kappa_1} a^\dagger a_p \\
 & + \sum_q (g_{1q} \sigma_{31} e^{i(\omega_p - \vec{k}_a \cdot \vec{v} - \omega_q)t} + g_{2q} \sigma_{32} e^{i(\omega_c - \vec{k}_c \cdot \vec{v} - \omega_q)t}) b_q \\
 & + \sum_r g_r d_r^\dagger a e^{i(\omega_r - \omega_p + \vec{k}_a \cdot \vec{v})t} + \text{h.c.}, \tag{3}
 \end{aligned}$$

where $\Delta_a = \omega_a - \omega_p$ represents the detuning of cavity mode and probe laser, $\Delta_p = \omega_3 - \omega_1 - \omega_p$ is the detuning of probe laser and the transition $|1\rangle \leftrightarrow |3\rangle$, and $\Delta_c = \omega_3 - \omega_2 - \omega_c$ is the detuning of the control laser and the transition $|2\rangle \leftrightarrow |3\rangle$.

Among the methods for open quantum systems [54–56], the Heisenberg-Langevin approach can faithfully reproduce the quantum dynamics. Especially, it can significantly reduce the complexity of calculation as compared to the widely-used quantum master equation [57, 58] and numerically-exact hierarchical equation of motion [59–61], when the system under investigation contains bosons and the number of operators of interest is small. In order to obtain the transmittance of the probe light, we apply

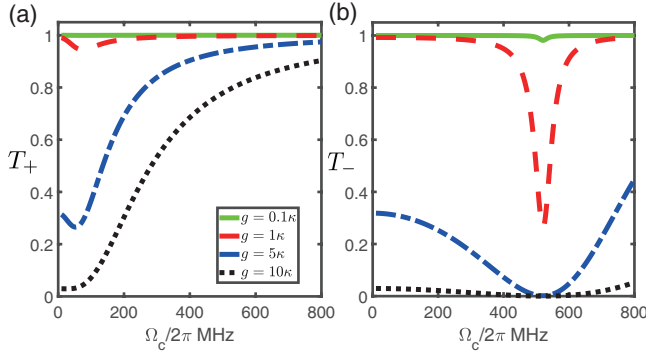


Figure 2: The transmittance vs the Rabi frequency Ω_c of the control field for the probe light in the (a) co-propagation, and (b) counter-propagation case, respectively. The green solid line refers to the case with $g = 0.1\kappa$, the red dashed line for $g = \kappa$, the blue dash-dotted line for $g = 5\kappa$, and the black dotted line for $g = 10\kappa$. The parameters are $v = 250$ m/s, $\Delta_a = \Delta_p = 0$, $\kappa_1 = 2\pi \times 0.5$ MHz, $\kappa_2 = 2\pi \times 4$ MHz, $\kappa_c = 2\pi \times 6$ MHz [25], $\gamma_3 = 2\pi \times 14.3$ MHz, and $\gamma_{12} = 10.6$ MHz [45].

the Heisenberg-Langevin approach to obtain

$$\dot{a} = -i(\Delta_a + \frac{\kappa}{2})a + \sqrt{\kappa_1}a_p - ig\sigma_{13} + F_a, \quad (4)$$

$$\begin{aligned} \dot{\sigma}_{13} = & -[\gamma_3 + i(\Delta_p + \vec{k}_a \cdot \vec{v})]\sigma_{13} - i\Omega_c\sigma_{12} \\ & + iga(\sigma_{33} - \sigma_{11}) + F_3, \end{aligned} \quad (5)$$

$$\begin{aligned} \dot{\sigma}_{12} = & -[\gamma_{12} - i(\Delta_p + \vec{k}_a \cdot \vec{v}) + i(\Delta_c + \vec{k}_c \cdot \vec{v})]\sigma_{12} \\ & - i\Omega_c\sigma_{13} + iga\sigma_{32} + F_2, \end{aligned} \quad (6)$$

where $\kappa = \kappa_1 + \kappa_2 + \kappa_c$, κ_1 (κ_2) is the coupling rate for the input (output) of the probe laser, and κ_c is the intrinsic damping rate of cavity, γ_3 is the spontaneous decay rate associated with the electronic excited state $|3\rangle$, and γ_{12} is the dephasing rate between the two ground states $|1\rangle$ and $|2\rangle$. F_a , F_3 , and F_2 are the Langevin noise operator of a , σ_{13} , and σ_{12} , respectively, which arise through the interaction with the reservoir, i.e.,

$$F_a = -i \sum_r g_r d_r(0) e^{-i(\omega_r - \omega_p)t}, \quad (7)$$

$$\begin{aligned} F_3 = & i \sum_q [g_{1q}(\sigma_{33} - \sigma_{11})b_q(0) e^{-i(\omega_q - \omega_p + \vec{k}_a \cdot \vec{v})t} \\ & - g_{2q}\sigma_{12}b_q(0) e^{-i(\omega_q - \omega_c + \vec{k}_c \cdot \vec{v})t}], \end{aligned} \quad (8)$$

$$\begin{aligned} F_2 = & i \sum_q [g_{1q}\sigma_{32}b_q(0) e^{-i(\omega_q - \omega_p + \vec{k}_a \cdot \vec{v})t} \\ & - g_{2q}\sigma_{13}b_q(0) e^{-i(\omega_q - \omega_c + \vec{k}_c \cdot \vec{v})t}]. \end{aligned} \quad (9)$$

Generally speaking, because the NV centers in nano-diamond interact with a complicated bath of phonons and spins, γ_3 and γ_{12} show dependence on various factors, e.g. the temperature, the magnetic field, and the density of magnetic impurities [62]. By generalization of cluster correlation expansion, we can numerically simu-

late the open quantum dynamics of the NV center in the presence of spin bath at the low temperature [63, 64].

The initial state of NV center is prepared at $|1\rangle$ by optical pumping [45]. Next, we consider the steady-state solution by setting $\langle \dot{a} \rangle = 0$, $\langle \dot{\sigma}_{13} \rangle = 0$, and $\langle \dot{\sigma}_{12} \rangle = 0$. In our configuration with $g \ll \Omega_c$, we have $\langle \sigma_{11} \rangle \approx 1$ and $\langle \sigma_{32} \rangle \approx 0$. Within the mean-field approximation, we have $\langle F_a \rangle = \langle F_3 \rangle = \langle F_2 \rangle = 0$. By setting $\Delta_a = \Delta_c = 0$ and solving Eqs. (4-6), we can obtain

$$\langle a \rangle_{\pm} = \frac{\sqrt{\kappa_1} \langle a_p \rangle}{i\Delta_p + \kappa/2 + i\chi_{\pm}}, \quad (10)$$

$$\chi_{\pm} = \frac{-i|g|^2}{\gamma_3 + i(\Delta_p + k_a v) + \frac{|\Omega_c|^2}{\gamma_{12} + i[\Delta_p + (k_a \mp k_c)v]}}, \quad (11)$$

where χ is the susceptibility of the NV center to the cavity mode, the subscript $+$ ($-$) corresponds to the co-propagation (counter-propagation) case. Due to the mutual movement of NV center and light, the Doppler effect can not be ignored. In our system, the control laser is always injected from the left side, while the probe laser can propagate in either the same or the opposite direction. As shown in Fig. 1, we shall only consider the component of the velocity which is parallel to the direction of light propagation for the Doppler effect. Therefore, as shown in Fig. 1 (a) and (c), assuming that both the control and probe fields are of the same wave length, we have $\vec{k}_c \cdot \vec{v} = kv$ for both cases, while $\vec{k}_a \cdot \vec{v} = kv$ for the co-propagation and $\vec{k}_a \cdot \vec{v} = -kv$ for the counter-propagation respectively.

According to the input-output theory [54, 55], the amplitude of the output field of the cavity is $\sqrt{\kappa_2} \langle a \rangle_+$ ($\sqrt{\kappa_1} \langle a \rangle_-$) in the co-propagation (counter-propagation) case. Thus, the transmission spectra for the co-propagation (counter-propagation) case T_+ (T_-) can be written as [55]

$$T_{\pm} = \left| \frac{\sqrt{\kappa_1 \kappa_2}}{i\Delta_p + \kappa/2 + i\chi_{\pm}} \right|^2. \quad (12)$$

By the contrast of the two transmittance defined as [65]

$$\eta = \frac{T_+ - T_-}{T_+ + T_-}, \quad (13)$$

we can evaluate the nonreciprocity of the rotating NV center.

III. NUMERICAL RESULTS AND ANALYSIS

We consider the nonreciprocal transport at the steady state. As shown in Fig. 2(a) for the co-propagation case with $v = 250$ m/s, e.g. a nano-diamond rotating at 1 GHz with an NV center located at radius $0.25 \mu\text{m}$ from the spin axis, we find a nearly-unity transport when $g \gg \kappa$ and Ω_c is large enough. This result demonstrates that

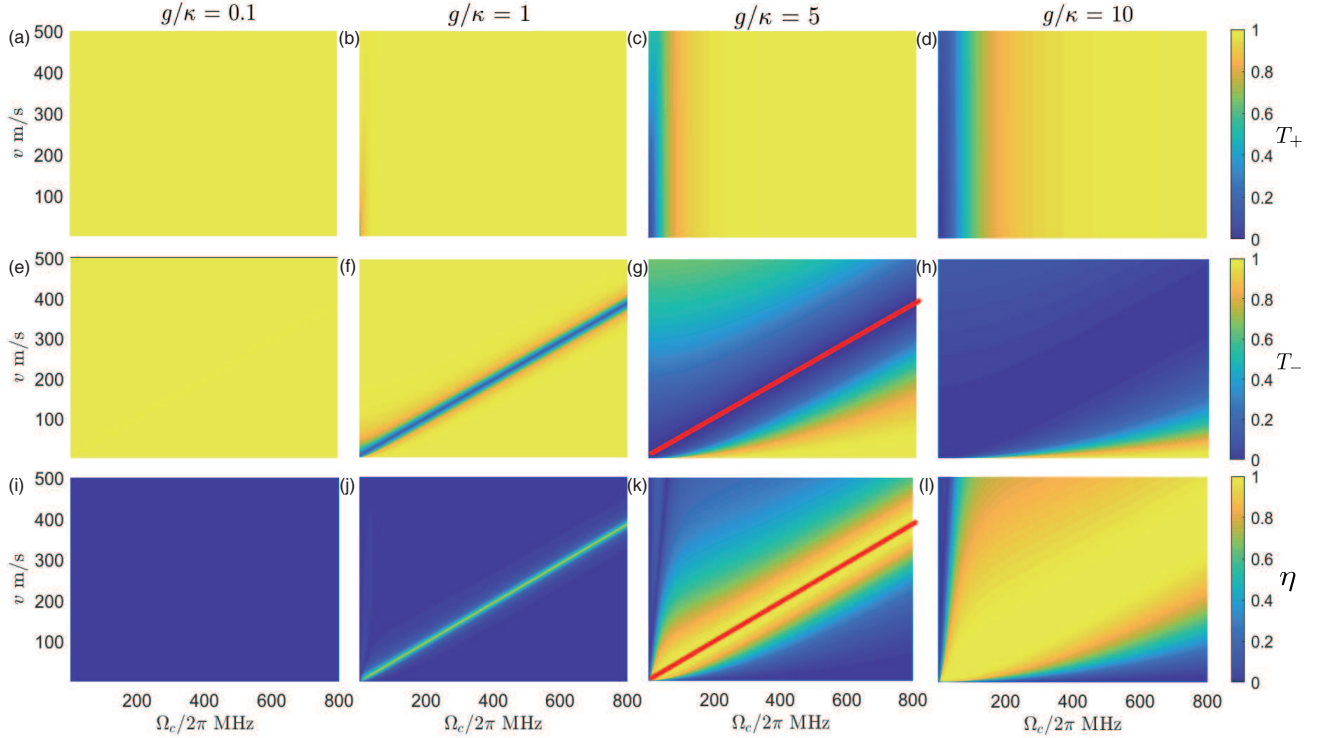


Figure 3: The relationship between the transmittance, contrast, the control field strength Ω_c and the velocity v . The top (middle) row corresponds to the transmittance T_+ (T_-) in the co-propagation (counter-propagation) case. The bottom row shows the contrast η . From left to right, each column corresponds to $g/\kappa = 0.1, 1, 5, 10$, respectively. The red lines in (g) and (k) is minimum value located at $kv = \sqrt{2}\Omega_c$.

the probe light explores the dark state for lossless transmission. In contrast, when the probe light propagates in the opposite direction of the control light, there is a fall around $\Omega_c = 500$ MHz. This fall becomes more profound when g is increased. Due to the term $2kv$ in χ_- of Eq. (11), χ_- should achieve a maximum value at some

Ω_c .

In order to investigate the underlying physical mechanism for the nonreciprocal transport, we explore the dark-state mechanism in Ref. [38]. The time evolution of the wave function is written as

$$|\psi(t)\rangle = -\frac{\Omega_c}{\Omega} e^{-i\frac{g^2}{\Omega^2}\omega_2 t} |E_1\rangle + \frac{g}{\sqrt{2}\Omega} e^{-\frac{i}{2}(\omega_1 + \frac{\Omega_c^2}{\Omega^2}\omega_2)t} (e^{-i\Omega t} |E_2\rangle + e^{i\Omega t} |E_3\rangle), \quad (14)$$

where $\Omega = \sqrt{g^2 + \Omega_c^2}$, $|E_j\rangle$'s are the three eigen states of the non-Hermitian system with $|E_1\rangle$ being the dark state and $|E_{2,3}\rangle$ being the bright states, $\omega_1 = \delta - i\gamma_3$ with δ being single-photon detuning, $\omega_2 = \Delta - i\gamma_{12}$ with Δ being two-photon detuning. The explicit expressions of the three eigen states are given as

$$|E_1\rangle \simeq \frac{1}{N_1} [(\omega_1\omega_2 - \Omega_c^2) |1\rangle - g\omega_2 |3\rangle + g\Omega_c |2\rangle], \quad (15)$$

$$|E_2\rangle \simeq \frac{1}{N_2} \{[(\Omega - \omega_1)(\Omega - \omega_2) - \Omega_c^2] |1\rangle + g(\Omega - \omega_2) |3\rangle + g\Omega_c |2\rangle\}, \quad (16)$$

$$|E_3\rangle \simeq \frac{1}{N_3} \{[(\Omega + \omega_1)(\Omega + \omega_2) - \Omega_c^2] |1\rangle - g(\Omega + \omega_2) |3\rangle + g\Omega_c |2\rangle\}, \quad (17)$$

with N_i 's being the normalization constants.

In our proposal, when the NV center is at rest, we set

two-photon resonance for the control and probe fields,

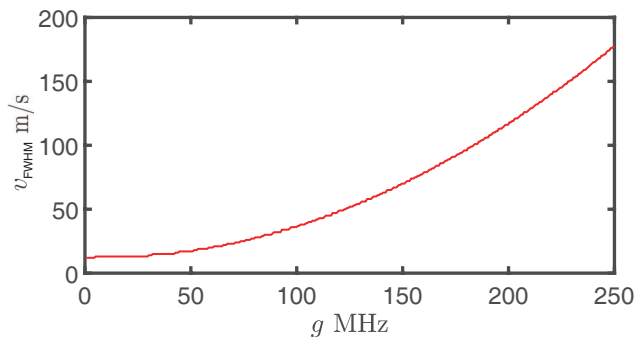


Figure 4: The velocity v_{FWHM} for the FWHM of η vs g in Fig. 3.

i.e., $\Delta = 0$. When the NV center rotates along with the nano-diamond, the Doppler shifts will arise for the two fields. In the co-propagating case, since the Doppler shifts will be the same, the two-photon resonance still holds. When $g \ll \Omega_c$, cf. Fig. 3(a)-(b), the probe field is immune to absorption because the dark state dominates, i.e., $\Omega_c/\Omega \simeq 1$, in the wave function, which decays at a lower rate of $(g^2/\Omega^2)\gamma_{12}$. If g is increased, cf. Fig. 3(c)-(d), two factors will enhance the absorption. On the one hand, because $\omega_1\omega_2 - \Omega_c^2 \ll g\omega_2, g\Omega_c$, $|2\rangle$ and $|3\rangle$ play a more significant role in $|E_1\rangle$. It makes the dark state more lossy, since it will decay at a larger rate as g is increased. On the other, the two bright states will make a greater contribution, about $g/\sqrt{2}\Omega$, to $|\psi(t)\rangle$ with a faster decay rate $(\gamma_3 + \kappa/2 + \Omega_c^2\gamma_{12}/\Omega^2)/2$. Therefore, we can observe a wider region for low transmittance as we increase g in Fig. 3(a)-(d).

If we turn to the counter-propagation case, we can observe a more interesting dependence of transmittance on v and Ω_c . When $g \ll \kappa$, as shown in Fig. 3(e), the transmittance is almost kept at unity for the whole parameter region. However, when $g = \kappa$ in Fig. 3(f), there emerges a dip in the transmittance for $kv = \sqrt{2}\Omega_c$. Along this line, we have $\omega_1\omega_2 - \Omega_c^2 \simeq 2(kv)^2 - \Omega_c^2 = 0$ and thus there is no component of $|1\rangle$ in $|E_1\rangle$. The main contribu-

tion from $|E_2\rangle$ and $|E_3\rangle$ in $|\psi(t)\rangle$ results in the lossy in the transmission. As g increases, this area of exception becomes wider. Interestingly, the width of the dip is almost not influenced by either v or Ω_c , but g . According to our numerical simulation as shown in Fig. 4, the velocity corresponding to the full width at half maximum of the contrast is proportional to g^2 .

IV. CONCLUSION AND DISCUSSION

In this paper, we explore the nonreciprocal transport in rotating nano-diamond induced by the EIT and the Doppler shift. We obtain the results at the steady state by the Heisenberg-Langevin approach. It is shown that the probe light makes use of the dark state and its transmission is generally not affected by the lossy intermediate state when it is incident in the same direction of the control light. However, the transmittance is significantly depressed around $kv = \sqrt{2}\Omega_c$ due to the breakdown of the two-photon resonance when the probe and control lights are in the opposite direction. Thus, we propose realizing optical nonreciprocity by using rotating nano-diamond with an NV center. We also discover that the velocity of the FWHM of contrast is proportional to g^2 .

Previously, it was experimentally shown that the energies of the electronic ground states of NV centers in diamond will be shifted due to the rotation as a result of Barnett effect [66–69]. However, since the energies of the electronic excited states will be correspondingly shifted by the same amount, the energy spectra in Fig. 1 will not be modified by the rotation. Thus, the above proposed nonreciprocal transmission in rotating nano-diamond with an NV center still holds.

We thank stimulating discussions with Jie-Qiao Liao, Jian Lin, and Yu-Qiao Li. This work is supported by the National Natural Science Foundation of China under Grant Nos. 11674033, 11474026, 11505007, and Beijing Natural Science Foundation under Grant No. 1202017.

-
- [1] M. Born and E. Wolf, *Principles of Optics* (Cambridge University Press, UK, 1999).
 - [2] D. Jalas, A. Petrov, M. Eich, W. Freude, S. Fan, Z. F. Yu, R. Baets, M. Popovic, A. Melloni, A. D. Joannopoulos, M. Vanwolleghem, C. R. Doerr, and H. Renner, What Is-and What Is Not-an Optical Isolator, *Nat. Photon.* **7**, 579 (2013).
 - [3] H. Kimble, The Quantum Internet, *Nature (London)* **453**, 1023 (2008).
 - [4] P. Lodahl, S. Mahmoodian, S. Stobbe, P. Schneeweiss, J. Volz, A. Rauschenbeutel, H. Pichler, and P. Zoller, Chiral Quantum Optics, *Nature (London)* **541**, 473 (2017).
 - [5] Y. Shoji, T. Mizumoto, H. Yokoi, I. W. Hsieh, and R. M. Osgood Jr., Magneto-Optical Isolator with Silicon Waveguides Fabricated by Direct Bonding, *App. Phys. Lett.* **92**, 071117 (2008).
 - [6] A. B. Khanikaev and A. Alù, Optical Isolators: Nonlinear Dynamic Reciprocity, *Nat. Photon.* **9**, 359 (2015).
 - [7] Z. F. Yu and S. H. Fan, Complete Optical Isolation Created by Indirect Interband Photonic Transitions, *Nat. Photon.* **3**, 91 (2009).
 - [8] S. Maayani, R. Dahan, Y. Kligerman, E. Moses, A. U. Hassan, H. Jing, F. Nori, D. N. Christodoulides, and T. Carmon, Flying Couplers above Spinning Resonators Generate Irreversible Refraction, *Nature (London)* **558**, 569 (2018).
 - [9] R. Huang, A. Miranowicz, J.-Q. Liao, F. Nori, and H. Jing, Nonreciprocal Photon Blockade, *Phys. Phy. Lett.*

- 121**, 153601 (2018).
- [10] J. F. Huang, Q. Ai, Y. G. Deng, C. P. Sun, and F. Nori, Atomic Blockade Induced by Photons inside Cavity, *Phys. Phys. A* **85**, 023801 (2012).
- [11] L. D. Tzuang, K. Feng, P. Nussenzeig, S. Fan, and M. Lipson, Non-Reciprocal Phase Shift Induced by an Effective Magnetic Flux for Light, *Nat. Photon.* **8**, 701 (2014).
- [12] A. B. Khanikaev, S. H. Mousavi, G. Shvets, and Y. S. Kivshar, One-Way Extraordinary Optical Transmission and Nonreciprocal Spoof Plasmons, *Phys. Rev. Lett.* **105**, 126804 (2010).
- [13] L. Bi, J. Hu, P. Jiang, D. H. Kim, G. F. Dionne, L. C. Kimerling, and C. A. Ross, On-Chip Optical Isolation in Monolithically Integrated Non-Reciprocal Optical Resonators, *Nat. Photon.* **5**, 758 (2011).
- [14] N. Bender, S. Factor, J. D. Bodyfelt, H. Ramezani, D. N. Christodoulides, F. M. Ellis, and T. Kottos, Observation of Asymmetric Transport in Structures with Active Nonlinearities, *Phys. Rev. Lett.* **110**, 234101 (2013).
- [15] L. Fan, J. Wang, L. T. Varghese, H. Shen, B. Niu, Y. Xuan, A. M. Weiner, and M. Qi, An All-Silicon Passive Optical Diode, *Science* **335**, 447 (2012).
- [16] L. Chang, X. Jiang, S. Hua, C. Yang, J. Wen, L. Jiang, G. Li, G. Wang, and M. Xiao, Parity-Time Symmetry and Variable Optical Isolation in Active-Passive-Coupled Microresonators, *Nat. Photon.* **8**, 524 (2014).
- [17] K. Fang, Z. Yu, and S. Fan, Realizing Effective Magnetic Field for Photons by Controlling the Phase of Dynamic Modulation, *Nat. Photon.* **6**, 782 (2012).
- [18] K. Fang, Z. Yu, and S. Fan, Photonic Aharonov-Bohm Effect Based on Dynamic Modulation, *Phys. Rev. Lett.* **108**, 153901 (2012).
- [19] F. Ruesink, M. A. Miri, A. Alù, and E. Verhagen, Nonreciprocity and Magnetic-Free Isolation Based on Optomechanical Interactions, *Nat. Commun.* **7**, 13662 (2016).
- [20] X. W. Xu and Y. Li, Optical Nonreciprocity and Optomechanical Circulator in Three-Mode Optomechanical Systems, *Phys. Rev. A* **91**, 053854 (2015).
- [21] X. W. Xu, L. N. Song, Q. Zheng, Z. H. Wang, and Y. Li, Optomechanically Induced Nonreciprocity in a Three-mode Optomechanical System, *Phys. Rev. A* **98**, 063845 (2018).
- [22] H.-Y. Zhu, X.-Y. Hu, J.-J. Lin, J.-Y. Wu, S. Li, Y.-X. Wang, F.-G. Deng, and N.-N. Zhang, Controllable Non-Reciprocal Transmission of Single Photon in Möbius Structure, *Ann. Phys. (Berlin)* **533**, 2100297 (2021).
- [23] C. Liang, B. Liu, A. N. Xu, X. Wen, C. C. Lu, K. Y. Xia, M. K. Tey, Y. C. Liu, and L. You, Collision-Induced Broadband Optical Nonreciprocity, *Phys. Rev. Lett.* **125**, 123901 (2020).
- [24] M. X. Dong, K. Y. Xia, W. H. Zhang, Y. C. Yu, Y. H. Ye, E. Z. Li, L. Zeng, D. S. Ding, B. S. Shi, G. C. Guo, and F. Nori, All-Optical Reversible Single-Photon Isolation at Room Temperature, *Sci. Adv.* **7**, eabe8924 (2021).
- [25] S. C. Zhang, Y. Q. Hu, G. W. Lin, Y. P. Niu, K. Y. Xia, J. B. Gong, and S. Q. Gong, Thermal-Motion-Induced Non-Reciprocal Quantum Optical System, *Nat. Photon.* **12**, 744 (2018).
- [26] G. W. Lin, S. C. Zhang, Y. Q. Hu, Y. P. Niu, J. B. Gong, and S. Q. Gong, Nonreciprocal Amplification with Four-Level Hot Atoms, *Phys. Rev. Lett.* **123**, 033902 (2019).
- [27] U. Fano, Effects of Configuration Interaction on Intensities and Phase-Shifts, *Phys. Rev.* **124**, 1866 (1961).
- [28] S. E. Harris, J. E. Field, and A. Imamoglu, Non-Linear Optical Processes Using Electromagnetically Induced Transparency, *Phys. Rev. Lett.* **64**, 1107 (1990).
- [29] M. O. Scully and M. S. Zubairy, *Quantum Optics* (Cambridge University Press, England, 1997).
- [30] M. Lobino, C. Kupchak, E. Figueroa, and A. I. Lvovsky, Memory for Light as a Quantum Process, *Phys. Rev. Lett.* **102**, 203601 (2009).
- [31] K. Honda, D. Akamatsu, M. Arikawa, Y. Yokoi, K. Akiba, S. Nagatsuka, T. Tanimura, A. Furusawa, and M. Kozuma, Storage and Retrieval of a Squeezed Vacuum, *Phys. Rev. Lett.* **100**, 093601 (2008).
- [32] A. M. Akulshin, S. Barreiro, and A. Lezama, Electromagnetically Induced Absorption and Transparency Due to Resonant Two-Field Excitation of Quasidegenerate Levels in Rb Vapor, *Phys. Rev. A* **57**, 2996 (1998).
- [33] M. Mücke, E. Figueroa, J. Bochmann, C. Hahn, K. Murr, S. Ritter, C. J. Villas-Boas, and G. Rempe, Electromagnetically Induced Transparency with Single Atoms in a Cavity, *Nature (London)* **465**, 755 (2010).
- [34] H. Dong, D. Z. Xu, J. F. Huang, and C. P. Sun, Coherent Excitation Transfer via the Dark-State Channel in a Bionic System, *Light: Sci. Appl.* **1**, e2 (2012).
- [35] L. Xu, Z.-R. Gong, M.-J. Tao, and Q. Ai, Artificial Light Harvesting by Dimerized Möbius Ring, *Phys. Rev. E* **97**, 042124 (2018).
- [36] N. Papasimakis, V. A. Fedotov, N. I. Zheludev, and S. L. Prosvirnin, A Metamaterial Analog of Electromagnetically Induced Transparency, *Phys. Rev. Lett.* **101**, 253903 (2008).
- [37] P. M. Anisimov, J. P. Dowling, and B. C. Sanders, Objectively Discerning Autler-Townes Splitting from Electromagnetically Induced Transparency, *Phys. Rev. Lett.* **107**, 163604 (2011).
- [38] Y.-Y. Wang, J. Qiu, Y.-Q. Chu, M. Zhang, J.-M. Cai, Q. Ai, and F.-G. Deng, Dark State Polarizing a Nuclear Spin in the Vicinity of a Nitrogen-Vacancy Center, *Phys. Rev. A* **97**, 042313 (2018).
- [39] H. J. Zhang, X. Y. Chen, and Z.-Q. Yin, Quantum Information Processing and Precision Measurement Using a Levitated Nanodiamond, *Adv. Quantum Technol.* **4**, 2000154 (2021).
- [40] M. W. Doherty, N. B. Manson, P. Delaney, F. Jelezko, J. Wrachtrup, and L. C. L. Hollenberg, The Nitrogen-Vacancy Colour Centre in Diamond, *Phys. Rep.* **528**, 1 (2013).
- [41] M.-J. Tao, M. Hua, Q. Ai, and F.-G. Deng, Quantum-Information Processing on Nitrogen-Vacancy Ensembles with the Local Resonance Assisted by Circuit QED, *Phys. Rev. A* **91**, 062325 (2015).
- [42] R. Schirhagl, K. Chang, M. Loretz, and C. L. Degen, Nitrogen-Vacancy Centers in Diamond: Nanoscale Sensors for Physics and Biology, *Ann. Rev. Phys. Chem.* **65**, 83 (2014).
- [43] L. S. Li, H. H. Li, L. L. Zhou, Z. S. Yang, and Q. Ai, Measurement of Weak Static Magnetic Fields with Nitrogen-Vacancy Color Center, *Acta. Phys. Sin.* **66**, 230601 (2017).
- [44] N. Zhao, J.-L. Hu, S.-W. Ho, J. T. K. Wan, and R. B. Liu, Atomic-Scale Magnetometry of Distant Nuclear Spin Clusters via Nitrogen-Vacancy Spin in Diamond, *Nat. Nanotech.* **6**, 242 (2011).
- [45] B. B. Zhou, A. Baksic, H. Ribeiro, C. G. Yale, F. Joseph Heremans, P. C. Jerger, A. Auer, G. Burkard, A. A. Clerk, and D. D. Awschalom, Accelerated Quantum

- Control Using Superadiabatic Dynamics in a Solid-State Lambda System, *Nat. Phys.* **13**, 330 (2017).
- [46] X. K. Song, Q. Ai, J. Qiu, and F. G. Deng, Physically Feasible Three-Level Transitionless Quantum Driving with Multiple Schrödinger Dynamics, *Phys. Rev. A* **93**, 052324 (2016).
- [47] X.-K. Song, H. Zhang, Q. Ai, J. Qiu, and F.-G. Deng, Shortcuts to Adiabatic Holonomic Quantum Computation in Decoherence-Free Subspace with Transitionless Quantum Driving Algorithm, *New J. Phys.* **18**, 023001 (2016)
- [48] M. P. Ledbetter, K. Jensen, R. Fischer, A. Jarmola, and D. Budker, Gyroscopes Based on Nitrogen-Vacancy Centers in Diamond, *Phys. Rev. A* **86**, 052116 (2012).
- [49] A. Ajoy and P. Cappellaro, Stable Three-Axis Nuclear-Spin Gyroscope in Diamond, *Phys. Rev. A* **86**, 062104 (2012).
- [50] Q. Ai, P.-B. Li, W. Qin, J.-X. Zhao, C. P. Sun, and F. Nori, NV-Metamaterial: Tunable Quantum Hyperbolic Metamaterial Using Nitrogen-Vacancy Centers in Diamond, *Phys. Rev. B* **104**, 014109 (2021).
- [51] R. Reimann, M. Doderer, E. Hebestreit, R. Diehl, and M. Frimmer, GHz Rotation of an Optically Trapped Nanoparticle in Vacuum, *Phys. Rev. Lett.* **121**, 033602 (2018).
- [52] J. H. Ahn, Z. J. Xu, J. H. Bang, Y.-H. Deng, T. M. Hoang, Q. K. Han, R.-M. Ma, and T. C. Li, Optically Levitated Nanodumbbell Torsion Balance and GHz Nanomechanical Rotor, *Phys. Rev. Lett.* **121**, 033603 (2018).
- [53] T. M. Hoang, Y. Ma, J. H. Ahn, J. H. Bang, F. Robicheaux, Z.-Q. Yin, and T. C. Li, Torsional Optomechanics of a Levitated Nonspherical Nanoparticle, *Phys. Rev. Lett.* **117**, 123604 (2016).
- [54] C. W. Gardiner, *Quantum Noise* (Springer, Berlin, 1991).
- [55] D. F. Walls and G. J. Milburn, *Quantum Optics* (Springer-Verlag, Berlin, 1994).
- [56] M.-J. Tao, N.-N. Zhang, P.-Y. Wen, F.-G. Deng, Q. Ai, and G.-L. Long, Coherent and Incoherent Theories for Photosynthetic Energy Transfer, *Sci. Bull.* **65**, 318 (2020).
- [57] H.-P. Breuer and F. Petruccione, *The Theory of Open Quantum Systems* (Oxford University Press, 2007).
- [58] Q. Ai, Y.-J. Fan, B.-Y. Jin, and Y.-C. Cheng, An Efficient Quantum Jump Method for Coherent Energy Transfer Dynamics in Photosynthetic Systems under the Influence of Laser Fields, *New J. Phys.* **16**, 053033 (2014).
- [59] A. Ishizaki and G. R. Fleming, Unified Treatment of Quantum Coherent and Incoherent Hopping Dynamics in Electronic Energy Transfer: Reduced Hierarchy Equation Approach, *J. Chem. Phys.* **130**, 234111 (2009).
- [60] B.-X. Wang, M.-J. Tao, Q. Ai, T. Xin, N. Lambert, D. Ruan, Y.-C. Cheng, F. Nori, F.-G. Deng, and G.-L. Long, Efficient Quantum Simulation of Photosynthetic Energy Transfer, *npj Quantum Inf.* **4**, 52 (2018).
- [61] N.-N. Zhang, M.-J. Tao, W.-T. He, F.-G. Deng, N. Lambert, and Q. Ai, Efficient Quantum Simulation of Open Quantum Dynamics at Various Hamiltonians and Spectral Densities, *Front. Phys.* **16**, 51501 (2021).
- [62] A. Jarmola, V. M. Acosta, K. Jensen, S. Chemerisov, and D. Budker, Temperature- and magnetic-field-dependent longitudinal spin relaxation in nitrogen-vacancy ensembles in diamond, *Phys. Rev. Lett.* **108**, 197601 (2012).
- [63] N. Zhao, S. W. Ho, and R. B. Liu, Decoherence and Dynamical Decoupling Control of Nitrogen-Vacancy Centre Electron Spins in Nuclear Spin Baths, *Phys. Rev. B* **85**, 115303 (2012).
- [64] Z. S. Yang, Y. X. Wang, M. J. Tao, W. Yang, M. Zhang, Q. Ai, and F. G. Deng, Longitudinal Relaxation of a Nitrogen-Vacancy Center in a Spin Bath by Generalized Cluster-Correlation Expansion Method, *Ann. Phys. (N.Y.)* **413**, 168063 (2020).
- [65] D. W. Wang, H. T. Zhou, M. J. Guo, J. X. Zhang, and S. Y. Zhu, Optical Diode Made from a Moving Photonic Crystal, *Phys. Rev. Lett.* **110**, 093901 (2013).
- [66] S. J. Barnett, Magnetization by Rotation, *Phys. Rev.* **6**, 239 (2009).
- [67] S. J. Barnett, Gyromagnetic and Electron-Inertia Effects, *Rev. Mod. Phys.* **7**, 129 (1935).
- [68] A. A. Wood, E. Lilette, Y. Y. Fein, V. S. Perunicic, L. C. L. Hollenberg, R. E. Scholten, and A. M. Martin, Magnetic Pseudofields in a Rotating Electron-Nuclear Spin System, *Nat. Phys.* **13**, 1070 (2017).
- [69] X.-Y. Chen, T. C. Li, Z.-Q. Yin, Nonadiabatic dynamics and geometric phase of an ultrafast rotating electron spin, *Sci. Bull.* **64**, 380 (2019).